CHAPTER IV

PROTEOMICS-BASED IDENTIFICATION OF ENOLASE 1 AS A POTENTIAL PROGNOSTIC MARKER IN CHOLANGIOCARCINOMA

4.1 Introduction

Cholangiocarcinoma (CCA) is a malignant tumor arising from the malignant transformation of cholangiocytes, the epithelial cells lining the biliary tree. CCA accounts for around 10–25% of the hepatobiliary malignancies in most parts of the world with age-standardized incidence rates (ASRs) between 0.3 and less than 1.5 per 100 000 in Western countries. However, the incidence in Thailand, where the key risk factor - the liver fluke *Opisthorchis viverrini* (*O. vivverrini*) is still endemic, is exceedingly high with ASRs of 33.4 per 100 000 in men and 12.3 per 100 000 in women (Sripa et al., 2008). People become infected by eating raw or undercooked freshwater fish in regional dishes that contain metacercarial stage of *O. viverrini*. It has long been known that infection with *O. viverrini* associate with the tumor initiation in the development of CCA (Sriamporn et al., 2004; Sriamporn et al., 2005; Sripa et al., 2007). This has led the World Health Organization's International Agency for Research on Cancer to classify *O.viverrini* as a Group 1 carcinogen to humans (Bouvard et al., 2009). Although mass anthelmintic therapy and intensive health education can protect individuals from being infected by *O.viverrini,* the early detection of CCA in those who have been infected by the fluke remains a challenge. CCA is characterized by a poor prognosis, with median survival of less than 24 months (Blechacz et al., 2008) and treatment options are limited. Surgical excision remains the mainstay of long-term survival for CCA but, unfortunately, the majority of patients are diagnosed at advanced stage, when surgical treatments are excluded. Hence there is a tremendous interest and urgency to identify novel CCA biomarkers for early diagnosis and prognostication.

In recent years, more and more attention has been drawn to the study of this deadly disease. Two-dimensional gel electrophoresis (2-DE) combining with mass

spectrometry (MS) is still the method of choice for the analysis of proteins above approximately 20-30 kDa. Although the technique itself is time consuming, difficult to reproduce and quantification, it can however be utilized in CCA research for the discovery of biomarkers as demonstrated by several groups(Srisomsap et al., 2004; Pak et al., 2009; Srisomsap et al., 2010). In our previous paper (Yonglitthipagon et al., 2010), we have reported on the membrane proteome analysis of four human *O. viverrini* associated CCA cell lines with a non-tumor H69 biliary cell line as a control using 2-DE and matrix assisted laser desorption ionization-time of flight-mass spectrometry (MALDI-TOF-MS). Peptide mass fingerprinting is a high-through put and sensitive method that has been commonly used for rapid screening of protein (Mortz et al., 1994). Using this method, we have identified annexin A2 (ANXA2) as a prognostic marker for predicting the poor outcome of CCA patients. In this study, we focused on a discovery of novel prognostic marker of bile duct cancer by investigation of differentially cytosolic protein profiles between four CCA cell lines with different tumor forming capabilities and H69 - a non-tumor biliary cell line as a control. We also discussed the prognostic significance of candidate protein found in human CCA tissues.

4.2 Materials and Methods

4.2.1 Cell cultures

Four human CCA cell lines, M156, K100, M139 and M213, were isolated from CCA patients from north eastern Thailand as described elsewhere (Sripa et al., 2005). In all cases, CCA was associated with chronic *O.viverrini* infection. Approval for use of the tissue was obtained from the Human Research Ethics Committee of Khon Kaen University, Thailand. CCA tissues were histologically diagnosed as follows: moderately differentiated adenocarcinoma (M156), poorly differentiated adenocarcinoma (K100), squamous cell carcinoma (M139), and adenosquamous cell carcinoma (M213). H69 cells, an 'immortalized' non-malignant human cholangiocyte cell line, and the CCA cell lines were cultured as previously described (Yonglitthipagon et al., 2010).

4.2.2 Cholangiocarcinoma tissue samples

In this study, CCA tissues were obtained after informed consent from the patients who underwent hepatectomy at Srinagarind hospital, Khon Kaen University, Thailand as described elsewhere (Yonglitthipagon et al., 2010). Of the 301 liver fluke-associated CCA samples analyzed, 203 were from males and 98 were from females at a ratio of 2:1. The mean (±SD) age in years was 55 ± 9.4 years (range, 31-75 years). Most of the patients were at an advanced CCA stage, 73.9% (n = 210) with lymphatic invasion, 53.1% (n = 152) with vascular invasion, and 39.6% (n = 112) with perineural invasion. The histopathologic grade of differentiation of the tumors was assessed to be well-differentiated histophotological type in 53 (35%) patients. The majority of patients (63.5%) possessed a tumor size > 5 cm.

4.2.3 Cytosolic protein preparation

The cell lines were examined under a phase-contrast microscope to ensure that they were over 70% confluence before lysis. The culture medium was discarded and the cells washed with 0.25 M sucrose three times on ice. Cells were scraped thoroughly with a scraper in 0.25 M sucrose containing 1% Protease Inhibitor Mix (GE Healthcare). The cells were collected and centrifuged at 1,500 ×g for 5 min at 4°C. The pellets were resuspended in lysis buffer containing 7 M urea, 2 M thiourea, 4% CHAPS, 2% IPG buffer pH 3-10 nonlinear (GE Healthcare), 40 mM DTT, and 1% Protease Inhibitor Mix and allowed to lyse on ice for 15 min. Cell lysates were sonicated according to the manufacturer's instructions (Sonics & Materials Inc. VCX 400, USA) and incubated for 2 h at 4°C. The lysate was then centrifuged at 600 ×g for 10 min to remove the nuclei and unlysed cells. The supernatant containing cytosolic protein was transferred to a clean tube and centrifuged at 10,000 ×g for 15 min to remove the mitochondrial fraction. The supernatant was collected again and centrifuged at 100,000 ×g for 2 h to generate a pellet containing the enriched microsomal fraction and the supernatant representing the cytosolic fraction. The total protein concentration in the cytosolic fraction was determined by Bradford Assay using a VersaMax™ absorbance microplate reader with SOFTMax pro (Molecular Devices Corporation California, USA) at 595 nm. Cytosolic proteins of each cell line were then ready for 2-DE.

4.2.4 2-DE of cytosolic proteins

Total cytosolic protein (100 μg) from CCA cell lines and H69 as a control were separated by 2-DE. Isoelectric focusing was performed using IPG strips (pH 3-10NL, 7 cm) on an IPGphor isoelectric focusing cell (GE Healthcare) and second-dimension SDS-PAGE using a Hoefer system (GE Healthcare) as described previously (Yonglitthipagon et al., 2010). After electrophoresis, the protein spots were visualized by CBR-250 (GE Healthcare) staining. Stained gels were scanned using an ImageScanner (GE Healthcare) and the 2-DE images of each cell line were compared using ImageMaster™ 2D Platinum 6.0 software (GE Healthcare).

4.2.5 Protein identification by MALDI-TOF-MS

Protein spots that were unique to or stained more intensely in CCA cell lines compared with H69 cells were excised from the gel and transferred to V-bottom 96-well microtitre plates. Tryptic digestions were performed on an EttanTM Spot Handling Workstation robot (Amersham Biosciences) according to the manufacturer's specifications. The 10 mg of matrix solution, α-cyano-4-hydroxycinnamic acid (Bruker Daltonik GmbH, Germany), was prepared by dissolving to saturation in 50% acetronitrile/water with 0.1% trifluoroacetic acid and then mixed with equal volumes of tryptic peptide with matrix solution. The mixture (1 μL) was spotted onto a steel target surface (MTP 384 ground steel, Bruker Daltonik) and dried at room temperature. Mass spectra were recorded on an Autoflex MALDI-TOF-mass spectrometer (Bruker Daltonik) at a maximum accelerating potential of 19 kV and in reflector mode. The *m/z* range was from 400 to 4000. The MALDI-TOF-MS was calibrated using trypsin auto-digestion peptide signals and matrix ion signals. Typically, 100 shots were accumulated from three to five different positions within a sample spot. The mass spectra were analyzed using MALDI evaluation software (Amersham Biosciences; release version 2.0). Proteins were identified by peptide mass fingerprinting using Mascot (http://www.matrixscience.com) in searches against the NCBInr (NCBInr 2009.04.03). The parameters used in the Mascot searches were as follows: (1) taxonomy was restricted to *Homo sapiens*, (2) trypsin specified with the allowance for one missed cleavage, (3) peptide mass tolerance fragment mass tolerance were set to 100 ppm and ± 0.5 Da, respectively and (4) carbamidomethyl and oxidized methionine were chosen as the fixed and variable modifications,

respectively. Protein hits were considered significant if the Mascot score was greater than 43 (significance level, $p < 0.05$). Other criteria for confident identification were that the protein match should have at least 17% sequence coverage and match at least 11 peptides. If peptides matched to multiple members of a protein family, proteins with shared peptides were grouped and the highest scoring protein was selected as the representative protein.

4.2.6 Tissue microarray and immunohistochemistry

Tissue microarrays (TMAs) were constructed by the Department of Pathology, Faculty of Medicine, Khon Kaen University, Thailand (Fedor et al., 2005). Prior to TMA construction, all tissue slides were histopathologically re-evaluated by experienced histopathologist (Chawalit Pairojkul). The extent of invasion by the cancer was determined in both the interface of the growing tumor border and the adjacent liver tissue. Pathologic vascular invasion was defined as the presence of a tumor cell emboli within a vessel space, which were identified by associated fibrin clot and/or an endothelial cell lining. Lymphatic invasion was defined as being present when cancer cells were detected floating within an endothelium-lined space. Perineural invasion was defined as tumor invading the perineural sheath or endoneurium.

Immunohistochemical (IHC) reactions were performed on 4 μm-thick sections of TMA silane-coated slides (Sigma, St. Louis, MO, USA) by an immunoperoxidase method as described (Yonglitthipagon et al., 2010). TMA sections probed with rabbit polyclonal anti-enolase 1 (Abcam Inc., USA) diluted 1:500 (v/v) diluted 1:400 (v/v) in PBS and incubated overnight at 4°C. After rinsing for 3x5 min with PBS the sections were incubated with horse radish peroxidase-conjugated goat anti-rabbit immunoglobulin (Zymed Labs, Carlsbad, CA) diluted 1:300 (v/v) in PBS and incubated at RT for 1 h. Sections were rinsed with PBS for 2x10 min, after which the sections were developed with DAB (Sigma Chemical Co.). The sections were counterstained with Mayer's haematoxylin, dehydrated, cleared in xylene and mounted in Permount®.

4.2.7 Assessment of immunohistochemistry and statistical analysis

Ponlapat Yonglitthipagon, Banchob Sripa and Chawalit Pairojkul who were blinded to patient status and outcome evaluated immunoreactivity independently. The percentage of positive tumor cells was determined using interactive stereological immunoscoring based on systematic random sampling (van Diest et al., 1997), and the mean score calculated. In this study, the percentage of positive cells expressing ENO1 was categorized as follows: <10% (-), ≥10% (+) as described elsewhere (Zhuang et al., 2008).

Statistical analyses of the data were performed with SPSS version 16.0 statistical package as described elsewhere (Yonglitthipagon et al., 2010). For cross-sectional analyses, the chi-square test was utilized to analyze the relationship between ENO1 expressions and categorical variables regarding clinical pathology parameters (e.g., age group, gender and histotype). The Kaplan–Meier method was used to calculate cumulative survival. Differences in survival between low expression and high expression groups were analyzed for significance by the log-rank method. The Cox-regression model was used to perform multivariate analysis, and values of $p < 0.05$ were considered statistically significant.

4.3 Results

4.3.1 2-DE of cytosolic proteins in H69 and CCA cell lines

In order to investigate the differential expression profile of cytosolic proteomes from cholangiocyte cell lines under non-tumor condition (H69) and in CCA (M156, KKU100, M139, three biological replicates for each cell type were generated. The separated protein spots were visualized on 2D gels by CBR-250 staining, and displayed good reproducibility for protein spot quantification and comparative analysis. Figure 4.1 shows representative 2-DE maps of each CCA cell lines (respectively M156, K100, M139 and M213) with spots subjected to MALDI-TOF MS and their identification numbers; the identified spots are listed in Table 4.1. The experimental p*I* and *Mr* values of identified proteins correlated with the theoretical values reported in the NCBInr database. The experimental p*I* and *Mr* values of identified proteins correlated with the theoretical values reported in the NCBInr database.

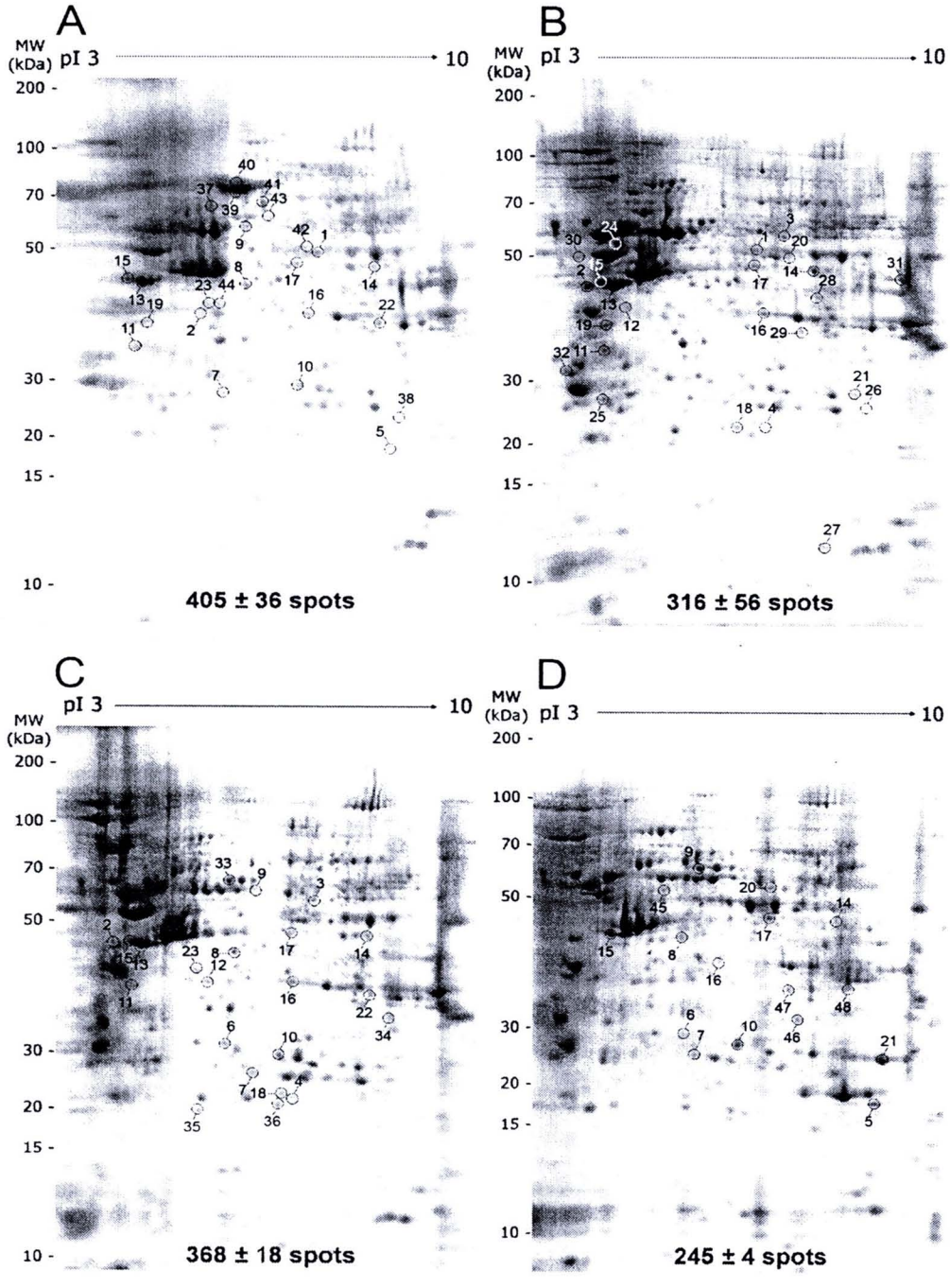

Figure 4.1 Comparative proteomic analysis of 2-DE gels of CCA cell lines; M156, moderately differentiated adenocarcinoma (A), KKU-100, poorly differentiated adenocarcinoma (B), M139, squamous cell carcinoma (C) and M213, adenosquamous cell carcinoma (D). Number of spots on 2-DE showed a total of 405±36, 316±56, 368±18 and 245±34 (mean±S.E. of three biological replicates) for the M156, KKU-100, M139 and M213, respectively.

Table 4.1 Total number of differentially expressed cytosolic proteins from 4 CCA cell lines identified by MALDI-TOF MS

No.[a]	A/N[b]	Description	Biological process	MS[c]	MP /TP[d]	CO[e]	*Mr*	p*I*	H69	M156	K100	M139	M213
1	gi|34147630	Tu translation elongation factor	Signal transduction	194	28 / 38	65	50.19	7.26	-	+	+	-	-
2	gi|1710248	Protein disulfide isomerase	Protein metabolic process	69	7 / 36	17	46.51	4.95	-	-	+	+	-
3	gi|169404695	Chain A, Pyruvate Kinase M2	Carbohydrate metabolic process	185	22 / 51	38	57.09	8	-	-	+	+	-
4	gi|544759	Biliverdin-IX beta reductase isozyme I	Unknown	110	10 / 27	51	21.96	7.31	-	-	+	+	-
5	gi|5031635	Cofilin 1	Cellular component morphogenesis	202	18 / 55	75	18.72	8.22	-	+	-	-	+
6	gi|4505773	Prohibitin	Nucleic and nucleotide metabolic process	211	17 / 42	73	29.84	5.57	-	+	-	+	+
7	gi|4758638	Peroxiredoxin 6	Oxygen and reactive oxygen species metabolic process	147	17 / 50	79	25.13	6	-	+	-	+	+
8	gi|119581639	Proteasome	Protein metabolic process	240	28 / 53	65	43.22	5.97	-	+	-	+	+
9	gi|4502643	Chaperonin containing TCP1	Protein metabolic process	306	38 / 80	65	58.44	6.23	-	+	-	+	+
10	gi|999892	Triosephosphate Isomerase	Carbohydrate metabolic process	220	19 / 42	84	26.81	6.51	-	+	-	+	+
11	gi|18314408	Nucleophosmin	Nucleic and nucleotide metabolic process	78	11 / 50	27	32.73	4.59	-	+	+	+	-
12	gi|15277503	ACTB protein	Cellular component morphogenesis	164	21 / 44	67	40.54	5.35	-	+	+	+	-
13	gi|62897681	Calreticulin	Protein metabolic process	222	20 / 38	58	47.06	4.3	-	+	+	+	-
14	gi|48145549	PGK1	Carbohydrate metabolic process	354	36 / 46	62	44.97	8.3	-	+	+	+	+
15	gi|90111766	Keratin 19	Cellular component organization	375	34 / 49	75	44.08	5.04	-	+	+	+	+

Table 4.1 Total number of differentially expressed cytosolic proteins from 4 CCA cell lines identified by MALDI-TOF MS (Cont.)

No.[a]	A/N[b]	Description	Biological process	MS[c]	MP /TP[d]	CO[e]	*Mr*	p*I*	H69	M156	K100	M139	M213
16	gi|119582950	Annexin A1	Intracellular protein transport	252	28 / 45	77	40.48	6.57	-	+	+	+	+
17	gi|203282367	Enolase 1	Carbohydrate metabolic process	174	21 / 44	53	47.35	6.99	-	+	+	+	+
18	gi|3023905	Glutathione S-transferase	Immune system process	148	12 / 34	57	23.64	6.89	-	-	+	+	-
19	gi|4502107	Annexin 5	Signal transduction	176	17 / 27	54	35.97	4.94	-	+	+	-	-
20	gi|197210452	Uridine monophosphate synthetase isoform I	Unknown	95	11 / 53	16	52.71	6.81	-	-	+	-	+
21	gi|4503727	FK506 binding protein 3, 25kDa	Negative regulation of apoptosis	109	12 / 38	44	25.22	9.26	-	-	+	-	+
22	gi|67464043	Human Liver Gapdh	Carbohydrate metabolic process	185	19 / 29	57	36.48	8.53	-	+	-	+	-
23	gi|82195535	Gamma-actin	Cellular component morphogenesis	165	22 / 50	64	42.09	5.3	-	+	-	+	-
24	gi|119602173	Heat shock protein 90kDa	Response to stress	117	16 / 35	27	57.87	4.92	-	-	+	-	-
25	gi|4507651	Tropomyosin 4 isoform 2	Cellular component organization	146	14 / 31	43	28.62	4.67	-	-	+	-	-
26	gi|21620034	ZSCAN21 protein	Nucleic and nucleotide metabolic process	43	12 / 20	24	26.69	9.45	-	-	+	-	-
27	gi|46409504	Hypothetical protein LOC400165	Unknown	46	42 / 82	38	13.69	8.66	-	-	+	-	-
28	gi|123266507	guanylatecyclase 1, soluble, beta 2	Nucleic and nucleotide metabolic process	44	39 /56	19	44.95	8.84	-	-	+	-	-
29	gi|7669492	Glyceraldehyde-3-phosphate dehydrogenase	Carbohydrate metabolic process	67	42 / 55	18	36.21	8.57	-	-	+	-	-

Table 4.1 Total number of differentially expressed cytosolic proteins from 4 CCA cell lines identified by MALDI-TOF MS (Cont.)

No.[a]	A/N[b]	Description	Biological process	MS[c]	MP /TP[d]	CO[e]	*Mr*	p*I*	H69	M156	K100	M139	M213
30	gi|5174735	Tubulin, beta, 2	Intracellular protein transport	148	23 / 36	57	50.26	4.79	-	-	+	-	-
31	gi|7108915	Glucocorticoid receptor AF-1	Signal transduction	69	42 / 85	19	46.58	9.08	-	-	+	-	-
32	gi|49119653	YWHAZ protein	Signal transduction	153	16 / 37	45	30.11	4.72	-	-	+	-	-
33	gi|189502784	Heat shock protein 60kD	Response to stress	249	30 / 48	59	60.81	5.83	-	-	-	+	-
34	gi|4504447	hnRNP A2/B1	Intracellular protein transport	89	19 / 46	44	36.04	8.67	-	-	-	+	-
35	gi|4507669	Tumor protein, translationally-controlled 1	Immune system process	116	16 / 41	61	19.69	4.84	-	-	-	+	-
36	gi|55960374	Transgelin 2	Muscle contraction	88	10 / 31	45	21.24	7.63	-	-	-	+	-
37	gi|31542947	Chaperonin	Protein metabolic process	230	26 / 50	52	61.19	5.7	-	+	-	-	-
38	gi|4505591	Peroxiredoxin 1	Oxygen and reactive oxygen species metabolic process	243	19 / 33	76	22.32	8.27	-	+	-	-	-
39	gi|46249758	Ezrin	Intracellular protein transport	258	28 / 31	43	69.31	5.94	-	+	-	-	-
40	gi|4505257	Moesin	Intracellular protein transport	146	26 / 46	33	67.89	6.08	-	+	-	-	-
41	gi|5803181	Hsp70/Hsp90	Response to stress	129	38 / 85	55	63.23	6.4	-	+	-	-	-
42	gi|52632385	hnRNP L	Nucleic and nucleotide metabolic process	104	13 / 28	35	51.16	7.22	-	+	-	-	-
43	gi|38013966	TKT protein	Lipid metabolic process	303	22 / 26	46	58.74	6.51	-	+	-	-	-
44	gi|167860126	Serine proteinase inhibitor	Protein metabolic process	278	25 / 42	73	42.53	5.72	-	+	-	-	-
45	gi|12803727	Keratin 7	Cellular component organization	210	22 / 33	46	51.44	5.42	-	-	-	-	+

Table 4.1 Total number of differentially expressed cytosolic proteins from 4 CCA cell lines identified by MALDI-TOF MS (Cont.)

No.[a]	A/N[b]	Description	Biological process	MS[c]	MP /TP[d]	CO[e]	*Mr*	p*I*	H69	M156	K100	M139	M213
46	gi|42476281	Voltage-dependent anion channel 2	Ion transport	147	13 / 25	54	32.06	7.49	-	-	-	-	+
47	gi|5174447	Guanine nucleotide binding protein	Intracellular protein transport	225	21 / 32	56	35.51	7.61	-	-	-	-	+
48	gi|54303910	Aging-associated gene 9 protein	Carbohydrate metabolic process	155	14 / 27	43	36.19	8.57	-	-	-	-	+

Note: [a]Numbers correspond to Figure 3.1. [b]NCBInr database accession numbers. [c]Mascot score (MS= -10*Log (P); where *P* is the pobability that the observed match is a random even from MS analysis. [d]The number of matched peaks/total peaks in MS analysis. [e]Percentage of sequence coverage. The presence of a protein in the relevant study is denoted with a '+' and the absence with a '-'.

4.3.2 MALDI-TOF-MS analysis of the differentially expressed spots

Using 2D gel replicates, identical and differential protein sports in 4 CCA cell lines subtracted from H69 were identified. In Table 1, the proteins, corresponding to 48 spots, which were expressed only in CCA cell lines but not in H69 are shown, together with the MS identification parameters. To classify the biological significance of the differentially expressed proteins, MS-identified proteins were classified into molecular and biological functional groups using the PANTHER database. Several of the identified proteins have been associated with cancer in previous studies, such as HSP60 (Desmetz et al., 2008), HSP70/HSP90 (Zhong et al., 2003), ezrin and moesin (Huang et al., 2010), and hnRNPs (David et al., 2010). As shown in Figure 4.2, representative mass spectra and the sequences of the assigned peptides for enolase 1 (ENO1) found in all CCA cell lines but not in H69. ENO1 was then selected for further verification, as its overexpression correlates with tumor transformation and invasion/metastasis in other cancers (Tsai et al., 2010; Zhang et al., 2010) but its prognostic implication in human *O. viverrini*-associated CCA tissues has not been explored.

A

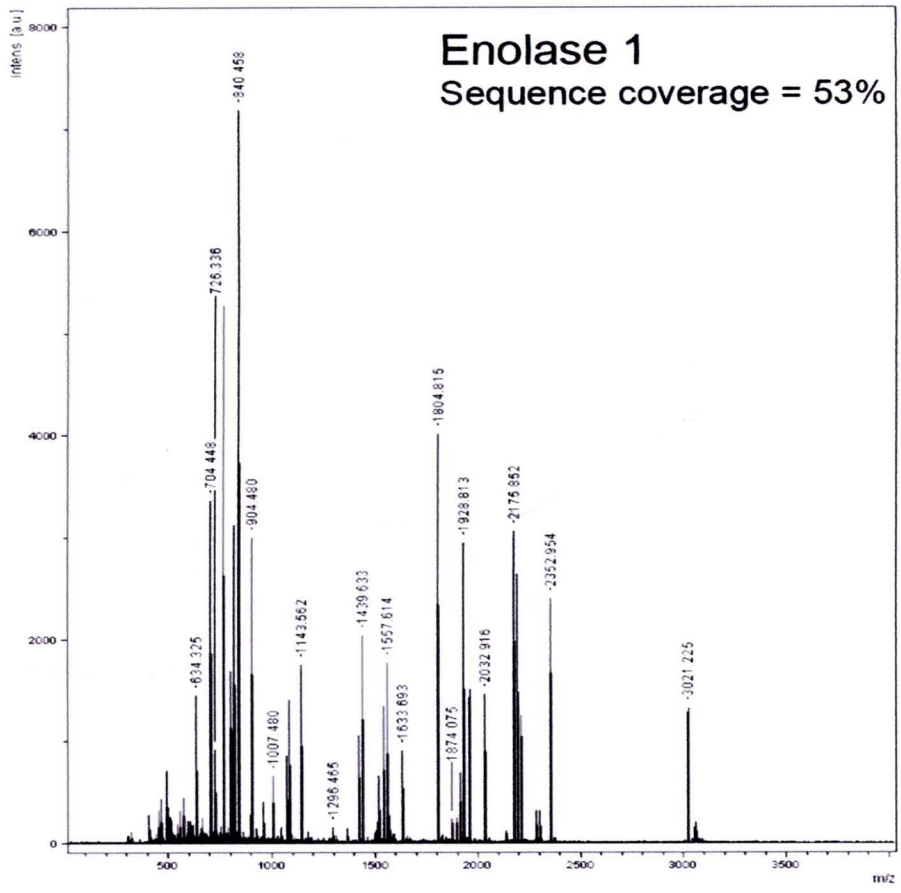

B

```
  1 SILKIHAREI FDSRGNPTVE VDLFTSKGLF RAAVPSGAST GIYEALELRD
 51 NDKTRYMGKG VSKAVEHINK TIAPALVSKK LNVTEQEKID KLMIEMDGTE
101 NKSKFGANAI LGVSLAVCKA GAVEKGVPLY RHIADLAGNS EVILPVPAFN
151 VINGGSHAGN KLAMQEFMIL PVGAANFREA MRIGAEVYHN LKNVIKEKYG
201 KDATNVGDEG GFAPNILENK EGLELLKTAI GKAGYTDKVV IGMDVAASEF
251 FRSGKYDLDF KSPDDPSRYI SPDQLADLYK SFIKDYPVVS IEDPFDQDDW
301 GAWQKFTASA GIQVVGDDLT VTNPKRIAKA VNEKSCNCLL LKVNQIGSVT
351 ESLQACKLAQ ANGWGVMVSH RSGETEDTFI ADLVVGLCTG QIKTGAPCRS
401 ERLAKYNQLL RIEEELGSKA KFAGRNFRNP LAK
```

Figure 4.2 Peptide mass fingerprint (PMF) of tryptic digests of enolase 1 obtained by MALDI-TOF MS. The spectrum displays *m/z* ratio (*x-axis*) and relative intensity (*y-axis*) of the peptides identified (A). Matched peptides of enolase 1 were 53% protein sequence coverage showed by red and underline (B). Protein identification using PMF data was performed with the Mascot search engine; acquired spectra were processed and search against the NCBInr database.

4.3.3 Immunolocalization of enolase 1 in CCA tissues

Once the role of enolase as a ligand for plasminogen, that has been reported to play a crucial role in invasion/metastasis, was selected for further verification. IHC studies were carried out on the TMAs (n = 301) to examine whether ENO1 expression changes during the development of bile duct cancer. The result showed weak staining of ENO1 was observed in the cytoplasm of corresponding normal liver tissue as shown in Figure 4.3A. In contrast, ENO1 was highly expressed in cytoplasm of hyperplastic bile duct (Figure 4.3B) and the majority of corresponding CCA tissues. Interestingly, IHC staining showed not only cytoplasmic but also membranous immunoreactivity. In addition, identification of perineural invasion (Figure 4.3C) and tumor emboli within lymphatic vessel (Figure 4.3D) detected by ENO1 immunohistochemistry was also observed.

4.3.4 Association of enolase 1 expression with clinical outcomes

To evaluate the relevance of ENO1 expression with clinicopathological outcomes of the patients, its expression status was quantified by interactive stereological immunostaining based on systematic random sampling (van Diest et al., 1997). The IHC showed that ENO1 was frequently overexpressed in CCA tissues, 74.75% (226/301) of biopsies stained positively. Statistical analysis showed that overexpression of ENO1 was significantly correlated with an age-related effect in young CCA patients ($\leq$ 56 years; p = 0.0001), a presence of lymphatic (p = 0.006) and an absence of perineural invasion (p = 0.006) shown in Table 2. No statistical differences in gender, histologic subtype, gross type, tumor size or tumor emboli observed within vascular vessel were found between patients with low or high ENO1 expression.

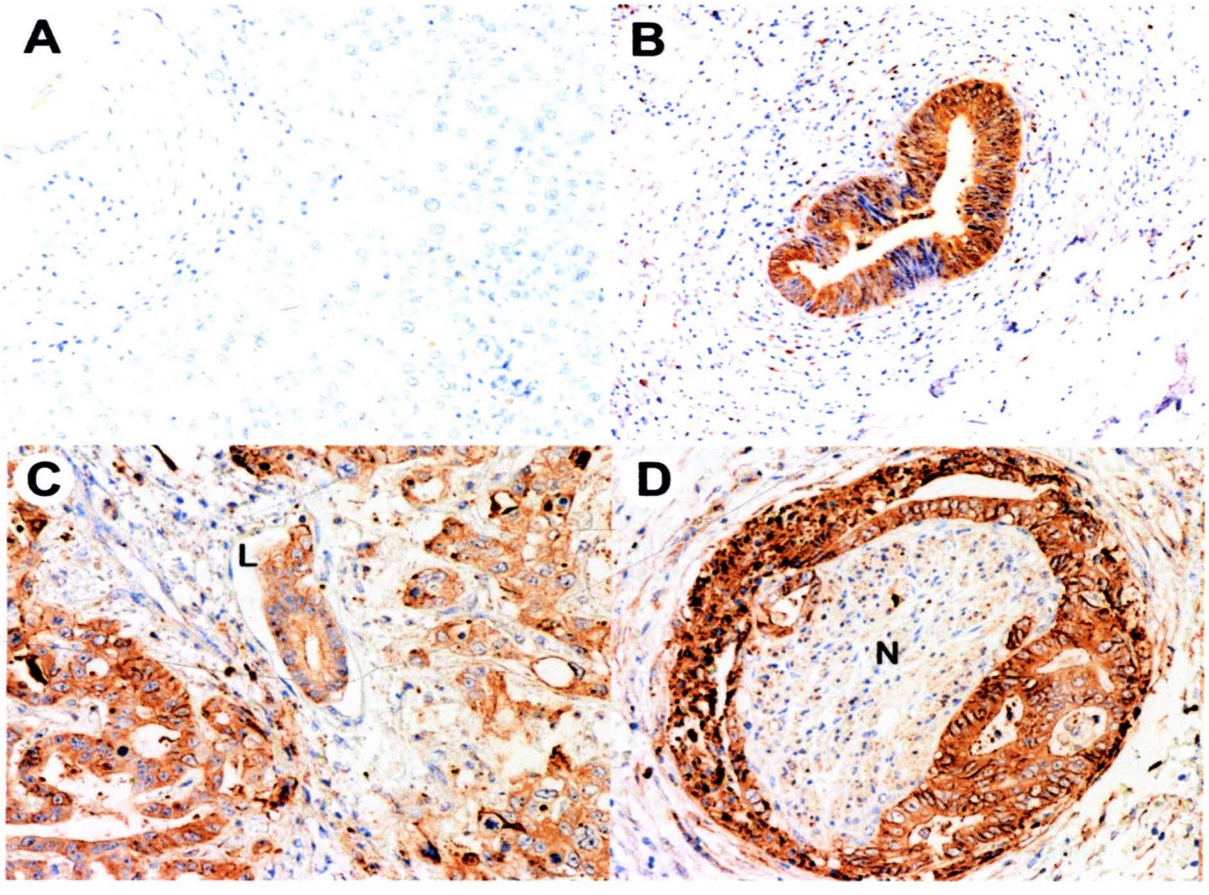

Figure 4.3 Immunohistochemistry of enolase 1 (ENO1) expression in normal bile duct epithelium and cholangiocarcinoma (CCA). Weak staining of ENO1 was observed in the cytoplasm of corresponding normal liver tissue (A). In contrast, ENO1 was highly expressed in cytoplasm of hyperplastic bile duct (B). In human CCA tissue, tumor with lymphatic permeation (C) and tumor with perineural invasion (D). Immunoperoxidase staining, original magnification × 100 (A-B), x 200 (C-D). L, lymphatic vessel; N, neural tissue.

Table 4.2 Clinicopathological variables and the expression status of enolase 1 (ENO1) in cholangiocarcinoma tissues

Variables	Enolase 1		*p*
	-ve	+ve	
Age (yr)			<0.0001
≤ 56	55	114	
> 56	19	111	
Gender			NS
Male	49	154	
Female	25	70	
Histotype			NS
Less diff.	57	181	
Well diff.	13	40	
Gross type			NS
Mass forming	36	106	
Periductal infiltrating	12	49	
Intraductal	2	7	
Tumor size			NS
≤ 5	20	54	
> 5	39	90	
Vascular invasion			NS
Absent	32	102	
Present	38	114	
Lymphatic invasion			0.006
Absent	27	47	
Present	43	167	
Perineural invasion			0.006
Absent	52	119	
Present	18	94	

Note: When the sum of subset numbers does not match patient totals, data were missing or unavailable. Tumor invasion in cholangiocarcinoma (CCA) tissues was diagnosed as positive if the patient fulfilled one of these three criteria: (i) vascular invasion; (ii) lymphatic invasion; or (iii) perineural invasion. NS indicates that the chi-square is not significant using the 0.05 threshold.

4.3.5 Expression of enolase 1 and cumulative survival

Survival analysis according to Kaplan-Meier method revealed significant correlation between ENO1 expression status and the survival in all patients (Figure 4.4). With log-rank test, we test the association between patients with high and low expression of ENO1. We found that patients with high ENO1 expression had much poorer survival than patients with low ENO1 expression (p = 0.004). The median length of survival for patients with high and low ENO1 expression was 28.14 weeks (95% CI, 22.74-33.54 weeks) and 44 weeks (95% CI, 26.72-61.28 weeks), respectively.

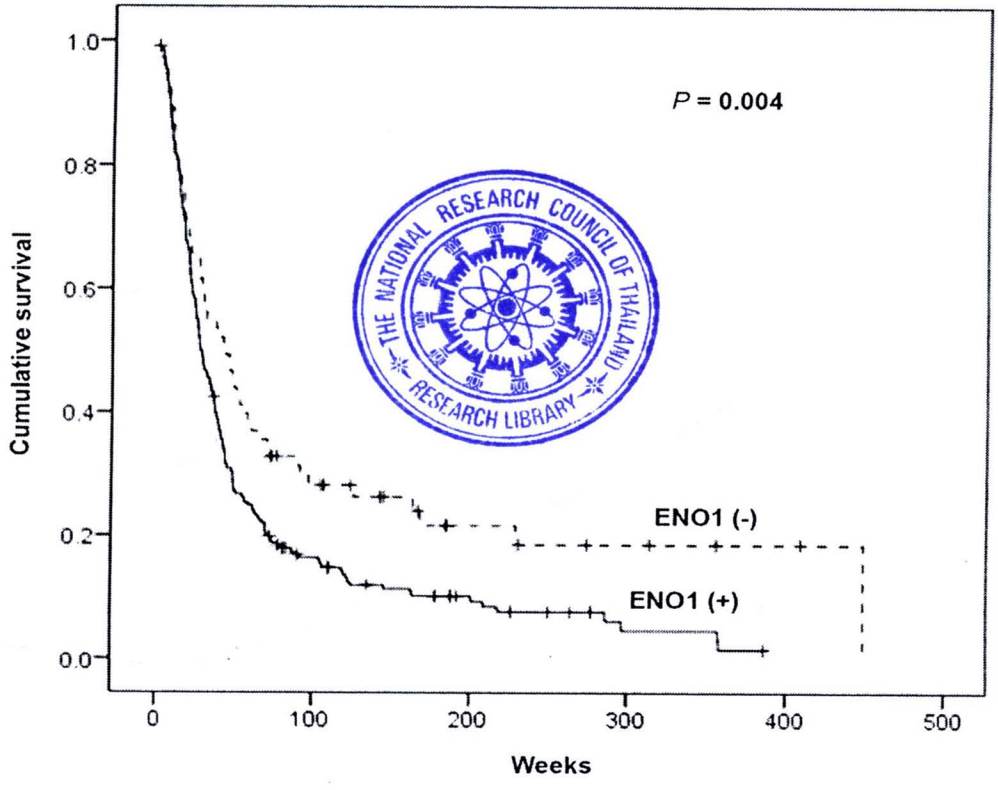

Figure 4.4 Kaplan-Meier cumulative survival curves of *Opisthorchis viverrini*-associated cholangiocarcinoma (CCA) patients categorized by the expression status enolase 1 (ENO1).

Cox multivariate analysis was used to test contribution of ENO1 expression status, age, gender, histologic subtype, gross type, tumor size and tumor invasion of the patients as shown in Table 4.3. High ENO1 expression proved to be associated with poor survival outcome (p = 0.001). Additionally, both tumor invasion and less-differentiated histologic subtype were identified as other factors contributing on poorer survival outcomes (p = 0.005 and p = 0.036, respectively). Taken together, these data strongly support expression status of ENO1 to be a potential prognostic marker for survival outcomes of CCA patients.

Table 4.3 Association between overall survival in patients with cholangiocarcinoma (CCA) and risk factors

Risk factors	Overall survival				
	Univariate analysis (Log-rank)		Multivariate analysis (Cox regression)		
	Median time, wk± SE (95% CI)	*p*	Relative risk	95%CI	*p*
Enolase 1		0.004			0.001
Absent	44±8.82 (26.716-61.284)		0.577	0.417-0.798	
Present	28.14±142.76 (22.74-33.54)		1		
Sex		0.03			NS
Male	27.14±1.74 (23.74-30.54)		0.762	0.572-1.016	
Female	40.14±4.22 (31.86-48.42)		1		
Tumor invasion		0.02			0.005
Absent	37.14±4.90 (27.54-46.74)		0.663	1.134-2.007	
Present	27.42±166 (24.17-30.67)		1		
Histology group		0.03			0.036
Less diff.	29.00±2.63 (23.85-34.15)		1.47	0.473-0.975	
Well diff.	41.14±6.47 (28.47-53.81)		1		

Note: CI, confident interval; NS, not significant.

4.4 Discussion

In this study, we applied a proteomics-based approach to identify differentially expressed tumor proteins in CCA cell lines. However, a drawback in using cell lines is that the cells are not representative of the tissue of origin because they have been maintained and propagated *in vitro* for extended time periods. Furthermore, each cell line was established from a few cells of a single patient biopsy, so cells may not accurately represent the tumor characteristics (Hay et al., 1988). Accordingly, validation of the cell line results in patient biopsies is essential.

We identified 47.35 kDa protein as human alpha-enolase (ENO1), which was identified in all CCA cell lines but not H69. About 75% of patients with CCA, we have examined thus far consistently show overexpression of ENO1 in hyperplastic bile duct and the tumors compared with that in tumor-adjacent normal tissue counterparts. Moreover, the statistical analyses correlating ENO1 expression in the patients with their clinicopathological outcomes further reveal that the expression status of ENO1 is highly associated with survival and tumor invasion of CCA patients. Regarding tumor invasion and less differentiated CCA in our multifactorial analysis, it has been previously reported that the survival time after surgery for the group with the presence of tumor invasion and metastasis was shorter than the group

with absence of tumor invasion and metastasis in CCA (Uttaravichien et al., 1999). Moreover, it was demonstrated that the patients with well differentiated CCA had longer survival times after surgery compared to less differentiated CCA (Nathan et al., 2007).

Enolase (EC4.2.1.11) is a glycolytic enzyme of approximately 47 kD and acts as a dimer containing Mg^{2+} responsible for catalyzing the conversion of 2-phosphoglycerate (2-PGE) to phosphoenolpyruvate (PEP) in the penultimate step of Embden Meyerhoff Parnas pathway (Jolodar et al., 2003). Verterbrates exhibit three tissue-specific enolase isozymes including α, β and γ-enolase (Bishop et al., 1990). α-enolase (enolase 1; ENO1) is found mainly in the liver although it is also present in other tissues, while β-enolase is abundant in muscles and γ-enolase is localized in neural tissues (Oliva et al., 1989).

Eukaryotic enolase 1 (ENO1) has been shown to be multifunctional proteins presenting a variety of activities besides their glycolytic activities (Pancholi, 2001). Overexpression of ENO1 is a common scenario in several cancers. In response to a number of stimuli, such as hypoxia, cytokine (interferon $\alpha_2\alpha_1$; INF$\alpha_2\alpha_1$) (Sousa et al., 2005a) and signals mediated by the MEK/ERK 1/2 pathway (Sousa et al., 2005b), normal cells will increase gene expression of ENO1 to adapt environmental stress through activation of hypoxic-inducible transcription factor. However, this cellular process is reversible for normal cells but irreversible for cancer cells. Additionally, tumor cells commonly use anaerobic glycolysis for inefficient energy metabolism (Warburg effect), leading to increase difficulties for disease treatment (Chang et al., 2006). Thus, elevated level of ENO1 expression may be involved in tumorigenesis.

ENO1 is also expressed on the cell surface and functions as a strong plasminogen-binding receptor, which may be involved in local fibrinolysis and contribute to tumor invasion (Redlitz et al., 1995). This is consistent with our finding that ENO1 was also detected on the cell surface of CCA, in addition to its presence in the cytosol. Hence, its dual location in cytosol and on cell surface indicated its pivotal role in glycolysis and tumor progression, respectively. However, the factors that affect its export and membrane association remain a mystery and are an important area for further research.

In conclusion, changes in energy metabolism are fundamental properties of cancer cells by which the cells survive in a state of hypoxic stress followed by promotion of angiogenesis and enhancement of local invasion or distal metastasis. In this study, overexpression of ENO1 in CCA patients is significantly associated with poorer clinical prognosis for survival. Coincidently, surface ENO1 also detected in the effusion tumor cells may implicate its potential role in cell invasion. Hence, ENO1 may be applied for a prognostic indicator for CCA patients.